The Journal of Experimental Biology 206, 771-784

doi:10.1242/jeb.00182

Mechanics of cuticular elastic energy storage in leg joints lacking extensor muscles in arachnids

Andrew T. Sensenig* and Jeffrey W. Shultz
Department of Entomology, University of Maryland, College Park, MD 20742, USA
*Author for correspondence (e-mail: sensenig@wam.umd.edu)

Accepted 29 November 2002

Summary

Certain leg joints in arachnids lack extensor muscles and have elastically deformable transarticular sclerites spanning their arthrodial membranes, an arrangement consistent with a model in which flexor muscles load transarticular sclerites during flexion and energy from elastic recoil is used for extension. This study quantifies the potential contribution of elastic recoil to extension torque at joints of the fourth leg of representative arachnids. Extension torques of isolated joints with and without transarticular sclerites were measured as the joint was rotated through angles and at angular velocities comparable with those used by walking animals. The procedure was repeated with the joint subjected to different internal fluid pressures in order to assess the potential role of hydraulically induced extension.

The efficiency of elastic energy storage (resilience) in the absence of internal fluid pressure was 70–90% for joints with well-developed transarticular sclerites, and the magnitude of torque was similar to those produced by different joint extension mechanisms in other arthropods. Increased internal fluid pressure acted synergistically with transarticular sclerites in some joints but had little or no effect in others. Joints that lacked both extensor muscles and transarticular sclerites appeared to be specialized for hydraulic extension, and joints operated by antagonistic muscles lacked apparent specializations for either elastic or hydraulic extension. It is well known that elastic energy storage is a significant contributor to propulsion in running vertebrates and certain arthropods, where elastic elements are loaded as the center of mass falls during one phase of the locomotor cycle. However, transarticular sclerites are apparently loaded by contraction of flexor muscles when the leg is not in contact with the substratum. Hence the mechanism of a transarticular sclerite is more similar to the flight and jumping mechanisms of other arthropods than to running vertebrates. The evolutionary significance and potential mechanical advantages of the transarticular elastic mechanism are discussed.

Key words: leg joint, extensor muscle, arachnid, transarticular sclerite, arthropod, elastic energy storage, resilience.

Introduction

Elastic energy-storage mechanisms (springs) are well known in arthropods, where they are important in generating forces for use in jumping (Bennet-Clark and Lucey, 1967; Evans, 1972, 1973; Bennet-Clark, 1975) and flight (Weis-Fogh, 1959; Alexander, 1988; Brodsky, 1994). These mechanisms consist of specific structures with unique material properties. The mechanics of running in cockroaches, centipedes and crabs suggest that energy is stored and released in a spring-like manner, but a specific structure involved in these energy exchanges has not been identified (Full, 1989; Blickhan and Full, 1993; Full and Koditschek, 1999). Those elastic structures that have been identified in the legs of pedestrian arthropods occur at distal joints and function in tarsal posture and movement (Radnikov and Bassler, 1991) or as antagonists to the claw rectractor muscle (Frazier et al., 1999; Neff et al., 2000). However, anatomical studies of arachnids (spiders, scorpions, mites, etc.) have revealed leg joints without extensor muscles, some of which have elastic transarticular sclerites spanning the arthrodial membranes connecting adjacent leg segments (Fig. 1) (Shultz, 1989, 1990, 1991). These observations suggest a propulsive mechanism in which energy is stored *via* deformation of the transarticular sclerites during flexion and recovered *via* elastic recoil during subsequent extension.

We examined the functional roles of elastic and hydraulic mechanisms in selected joints from the fourth walking leg of several arachnid groups, including scorpions (Scorpiones), tarantulas (Araneae), whipscorpions (Uropygi), sun-spiders (Solifugae) and harvestmen (Opiliones). Measurements were taken by recording forces exerted by each joint during mechanically induced joint movements approximating those used by walking animals. These organisms exhibit a diverse range of leg adaptations for extension and were expected to differ significantly in mechanics. For example, scorpions have evolved a muscle that functions in extension of major leg joints, and tarantulas and whipscorpions are known to make

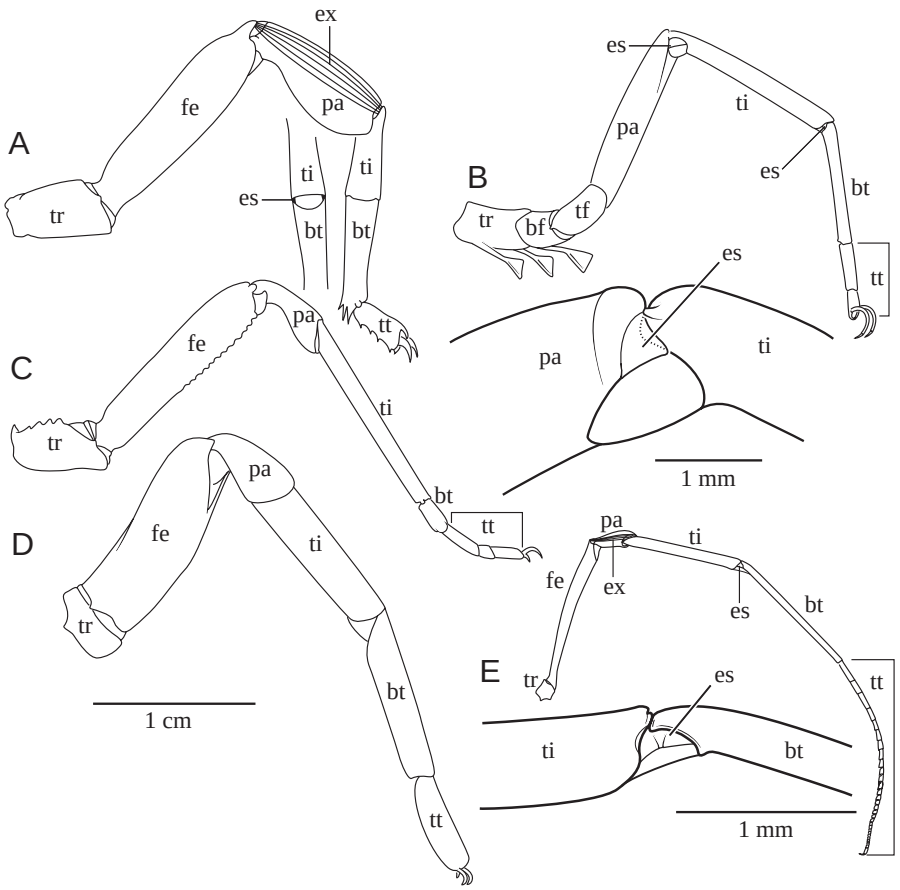

Fig. 1. Fourth walking legs of arachnids, showing their basic anatomy. Whole legs are shown at approximately the same scale. (A) *Heterometrus*; left leg, anterior perspective, inset showing posterior perspective. (B) *Eremopus*; right leg, posterior perspective, inset showing elastic sclerite of patella–tibia joint. (C) *Mastigoproctus*; left leg, anterior perspective. (D) *Aphonopelma*; right leg, posterior perspective. (E) *Leiobunum*; right leg, posterior perspective, inset showing elastic sclerite of tibia–basitarsus joint. bf, basifemur; bt, basitarsus; es, elastic sclerite; ex, extensor muscle; fe, femur; pa, patella; tf, telofemur; ti, tibia; tr, trochanter; tt, telotarsus.

wide use of hydraulic pressure. Sun-spiders have large transarticular sclerites on two important leg joints, while in harvestmen these are found on only one leg joint.

The magnitude of the torque generated by an elastic mechanism was measured to evaluate the degree to which the animal relies on elastic extension as the sole or primary extensor of a joint. Torque generated by hydraulic pressure was compared with that generated by elastic extension mechanisms, and changes in internal joint volume with joint angle were used to indicate the possible use of hydraulic pressure. The dynamic context of locomotion required examination of frequency effects on both resilience and torque. Finally, the energy contribution by elastic extension to propulsion in the arachnids used in this study can be compared with muscular extension in a commonly studied arthropod, the cockroach *Blaberus discoidalis*.

Materials and methods

Animals and anatomy

Animals used in this study included sun-spiders (*Eremopus gigasellus*, Solifugae) (N=6, mass 1.4±0.4 g), tarantulas (*Aphonopelma seemani*, Araneae) (N=4, mass 16±5 g), desert hairy scorpions (*Hadrurus arizonensis*, Scorpiones: Iuridae) (N=6, mass 6.5 ± 1.4 g), Asian forest scorpions (*Heterometrus spinifer*, Scorpiones: Scorpionidae) (N=7, mass 7.6±1.0 g), giant whipscorpions (*Mastigoproctus giganteus*, Uropygi) (N=7, mass 6.2±1.6 g) and harvestmen (*Leiobunum formosum*, Opiliones) (N=8, mass 77±12 mg). *Eremopus*, *Aphonopelma*, *Mastigoproctus*, *Hadrurus* and *Heterometrus* were housed in plastic shoe boxes. Water was provided *ad libitum* in either open Petri dishes or glass vials plugged with cotton wool, and animals were fed one cricket per week for several weeks. *Leiobunum* were kept in a large terrarium on a layer of moistened soil and fed oatmeal. After kinematic analysis of walking was completed, animals were killed by freezing to –80°C and maintained at this temperature until used in an experiment. Joints of fresh animals and of those previously frozen showed no change in basic material properties.

The study was conducted on selected joints of the fourth (most posterior) walking leg (Fig. 1). This leg functions primarily in pushing the animal forward by joint extension. We focused on bicondylar hinge joints (one axis of movement), which undergo substantial angular excursions during locomotion, rather than monocondylar joints (multiple axes of movement) or joints that show little movement during locomotion. Based on these criteria, we examined the femur–patella joints in scorpions, *Mastigoproctus* and *Aphonopelma*; the patella–tibia joints in scorpions, *Eremopus* and *Mastigoproctus*; the tibia–basitarsus joint in all taxa; and the basitarsus–telotarsus joint in *Aphonopelma*. Elasticity appeared in some other distal joints but movement was complex, limited in range, or did not occur in forward locomotion and thus these joints were examined superficially.

Kinematic analysis

Each animal was videotaped as it walked on a variable-speed treadmill (treadmill dimensions, 50 cm×20 cm length×width, speed resolution, 5 mm s^{-1}). Images of walking animals were captured using two gen-locked Peak Performance High Speed cameras (60 fields s^{-1} for *Eremopus* and *Leiobunum* and 60 or 120 fields s^{-1} for *Aphonopelma*, *Hadrurus*, *Heterometrus* and

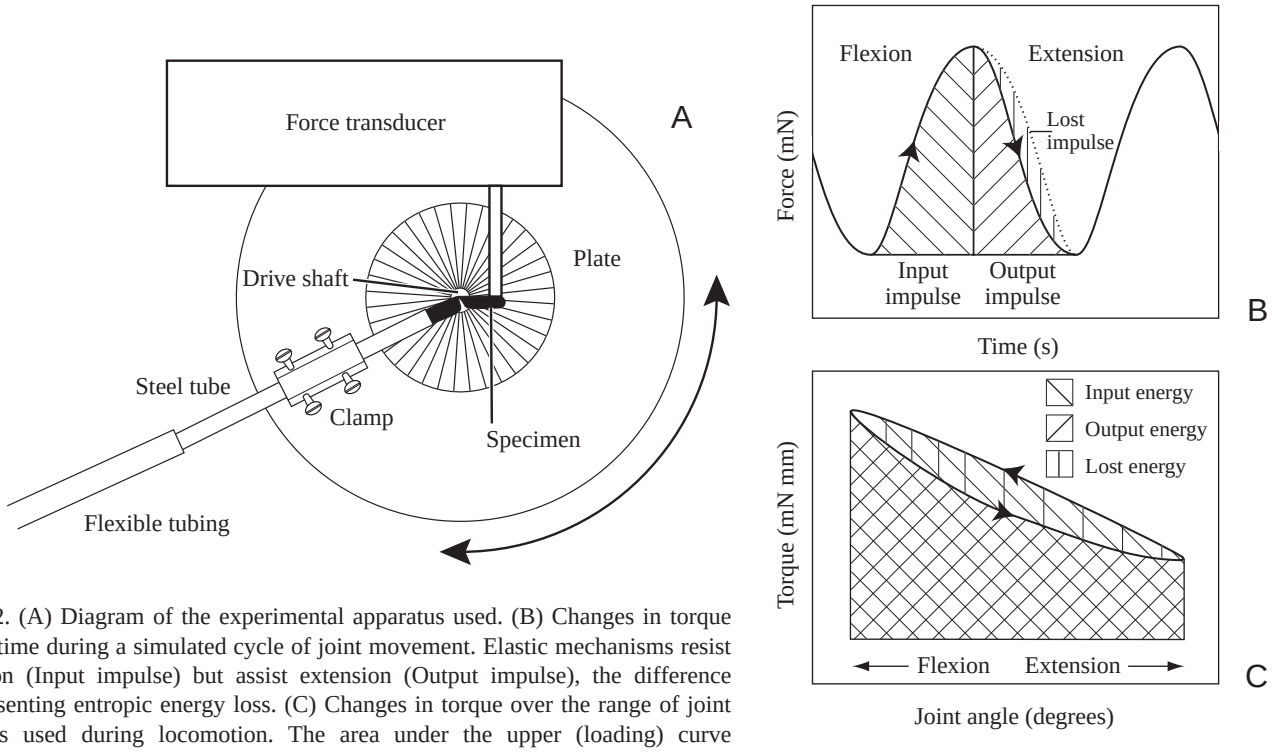

Fig. 2. (A) Diagram of the experimental apparatus used. (B) Changes in torque over time during a simulated cycle of joint movement. Elastic mechanisms resist flexion (Input impulse) but assist extension (Output impulse), the difference representing entropic energy loss. (C) Changes in torque over the range of joint angles used during locomotion. The area under the upper (loading) curve represents input energy; the area under the lower (unloading) curve represents output energy; the difference between them represents lost energy. Output energy divided by input energy multiplied by 100 is the percent efficiency or resilience.

Mastigoproctus), positioned so as to obtain lateral and dorsal perspectives of the animal. The angle between the cameras ranged from 60–90°. The videotapes were synchronized using the Peak Performance manually operated event marker. A calibration frame (4 cm×4 cm×4 cm or 25 mm×15 mm×11 mm) was videotaped by both cameras. The larger frame consisted of 12 non-coplanar points and the smaller frame 6 non-coplanar points. The smaller calibration frame was used for smaller animals. The resolution of points of the calibration frames was approx. 0.5 mm. Using the larger calibration object, points in space could be located with mean-squared errors of 0.09 mm, 0.23 mm and 0.35 mm for the *x*, *y* and *z* positions, respectively, yielding a 0.43 mm mean-squared error for position. Using the smaller calibration object, points in space could be located with mean-squared errors of 0.023 mm, 0.136 mm and 0.103 mm for the *x*, *y* and *z* positions, respectively, yielding a 0.172 mm mean-squared error for position. Paint was used to mark the articulations of the fourth leg to facilitate subsequent digitization.

Videotapes of walking animals were analyzed to determine the natural range of motion at each joint using a computerized motion analysis system (Motus, Peak Performance Technologies, Inc., version 6.0). Video images were digitized manually. Data were filtered using a low-pass, fourth-order, zero-phase-shift Butterworth digital filter with a cut-off frequency of 10 Hz, a frequency that minimized distortion and noise (Biewener and Full, 1992). Data from both camera views were filtered before direct linear transformation to three-dimensional coordinates in Motus.

Mechanically controlled joint movement and kinetic analysis

A computer-controlled stepper motor (Arrick Robotics, Model MD-2, angular resolution of motor 0.9° step^{-1}, angular resolution of plate shaft achieved through gearing 0.75° step^{-1}) was used to belt drive a shaft terminating with a flat circular plate equipped with a specimen clamp (Fig. 2A). The stepper motor was programmed to rotate the plate through angular excursions and velocities approximating those observed during locomotion (position *versus* time was linear, i.e. a saw-tooth wave). A rotary variable-inductance transducer (Schaevitz, Model RVIT-15-60, linearity error 0.25% full-scale output) was mounted on the same shaft as the plate and used to record the instantaneous angle. The stepper motor, belt, gears, plate and rotary transducer were mounted together in a stiff steel frame. A force transducer (Aurora Scientific Inc, Model 404A, range 100 mN, resolution 2000 nN) was attached to a separate laboratory stand and the transducer input tube was brought into contact with the free end of a clamped and mounted joint specimen (Fig. 2A). The transducer measured the force exerted at the free end of the joint during mechanically induced flexion and extension. Force and angular position data were collected using an Analog/Digital Interface Unit and Motus 6.0 software (Peak Performance Technologies) at a sampling rate of 600 Hz. Joints were rotated through 0.5, 1, 2, 3.3, 5 and 10 Hz. Force data were filtered in the Motus program using a Butterworth filter (cutoff frequency 6–12 Hz). The cutoff frequency for each trial was chosen so that approximately equivalent noise reduction occurred among trials of different rotation frequencies.

Joint preparation

Each joint was prepared by thawing an animal from –80° C, amputating a fourth leg, isolating the experimental joint by cutting away portions of the leg segments proximal and distal to the joint, removing all muscles and tendons, and mounting one end of the joint specimen at the end of a stainless steel tube (5 mm diameter, 6 cm length) (Fig. 2A). Epoxy resin was used to seal the specimen–tube interface and the free end of the joint specimen was also sealed with epoxy. The epoxy was allowed to dry for approx. 30 min, and the joint and tube were filled with Ringer's solution (Ingham and Jowett, 1997). A long micropipette was inserted into the steel tube and used to inject the solution, a procedure intended to ensure that the specimen was filled and that air bubbles in the joint and tube were minimized.

The stainless steel tube was clamped to the plate so that the joint axis could be aligned with the shaft axis by eye (Fig. 2A). Adjustments were made using the clamp screws to ensure that joint movement was in a plane parallel to the plate surface. The force transducer input tube was brought into direct contact with the joint at a right-angle to the free end of the joint specimen. The point of contact between the specimen and transducer was improved when necessary by scraping off setae or applying a drop of melted paraffin. A protractor next to the plate allowed positioning of the joint angle by eye (resolution approximately 5°), the stepper motor was turned on and locked at this angle, and all angular excursions were then based on this start position. Errors in torque measurement were caused primarily by misalignment of the joint and shaft axes, and secondarily by precision in positioning the starting joint angle. The stainless steel mounting tube was then attached through rubber tubing to a graduated titration cylinder (length 50 cm) to which Ringer's solution was added. Fluid pressure was varied by changing the vertical placement of the cylinder relative to the joint specimen. The arthrodial membrane was observed prior to cycling to ensure that fluid was filling the specimen. Internal fluid pressures of 0, 2.5, 4.9 and 9.8 kPa were applied to encompass the range of pressures typically measured in walking and resting arachnids, although much higher pressures have been measured in startled and restrained animals (for example, see Alexander, 1967; Stewart and Martin, 1974; Anderson and Prestwich, 1975; Blickhan and Barth, 1985; Shultz, 1991). To ensure that bubbles trapped in joints with transarticular sclerites were not the main mechanism generating elastic properties, torque generated by empty joints (joints with muscles removed but not yet connected to flexible tubing and filled with solution) was measured and was found to be essentially the same as those filled with solution. While drying of the arthrodial membrane will eventually result in an empty joint becoming completely stiff, increased stiffness of empty joints was not apparent until several hours had elapsed.

Measurement of changes in joint volumes

Use of internal pressure for joint extension should be correlated with an increase in joint volume during extension (Blickhan and Barth, 1985); absence of volume increase indicates the absence of hydraulically mediated extension. Changes in joint volume during flexion and extension were measured by observing fluid movement in a micropipette attached to the joint mounting tube. A 50 µl micropipette was marked with 1 µl increments and glued to a 3 cm piece of flexible tubing. The flexible tubing was then attached to the steel mounting tube. Filling and assembly of components were performed in a pan of saline to minimize the presence of air bubbles. The joint specimen was held lower than the micropipette so as to increase the pressure in the joint by approx. 2.5 kPa (18 mmHg) and the joint was flexed and extended by hand. The precision of this technique was approx. 0.5 µl.

Calculations of torque and efficiency of elastic energy storage

Data sets were imported to a spreadsheet program (Microsoft Excel 97). Scaled (or relative) torque (τ_s) of a joint was calculated according to Evans and Forsythe (1984):

$$\tau_s = flm^{-0.67}, \quad (1)$$

where f is force in mN, l is lever arm in mm and m is mass of the animal in g. The scaling exponent –0.67 reflected the assumptions that muscle force is proportional to muscle cross-sectional area and that the skeletomuscular system scales isometrically (Evans and Forsythe, 1984). Scaled torque generated at the angle midway between maximum flexion and maximum extension (from kinematic analysis) was considered a reasonable value for quantitative comparison of animals. Torque at this angle is a more meaningful comparison than maximum torque, because it is not as dependent on the angle of maximum flexion and the resolution of this angle. Statistical differences between the means of midrange scaled torque were determined using *t*-tests.

Elastic energy storage was measured by flexing and extending individual joints under zero internal fluid pressure while recording the input and output impulse. Input impulse was calculated as the area under the loading curve (flexion) in the torque–angle graph (Fig. 2B,C), while output impulse due to elastic recoil was the area under the unloading curve (extension). Areas under these curves were calculated using a Visual Basic program in Microsoft Excel 97 that summed all torque values between a minimum and a maximum in the loading curve (sampling frequency 600 Hz). The percentage efficiency of elastic energy storage (or resilience) was calculated as (output impulse/input impulse)×100. The curves obtained by manipulating joints under zero internal pressure were compared to those obtained with the joint under various positive fluid pressures, but the resilience obtained under these conditions represented the relative effectiveness with which the joint transduced internal fluid pressure into kinetic energy during flexion and extension in addition to resilience.

Calculation of potential contribution of elastic recoil to propulsion

The potential propulsive work contributed by elastic recoil

of a joint was calculated from kinematic data obtained by video analysis of walking animals and kinetic data from force measurements on isolated joints under zero internal fluid pressure. Potential work (W) directly contributed by recoil to forward motion of the animal's center of mass during one propulsive stroke was calculated using the following equation:

$$W = \int F\,dx \approx \int \tau(\theta)\sin(\theta)tv(\theta_{start}-\theta_{end})^{-1}\,l^{-1}d\theta\,, \qquad (2)$$

where θ is the contact angle (i.e. the projection onto the sagittal plane of the angle between the lever arm and the substratum), θ_{start} is the angle at the onset of the propulsive stroke, θ_{end} is the angle at the end of the propulsive stroke (all angles in degrees), t is the duration of the propulsive stroke in s, v is the average speed of the center of mass in the direction of travel in mm s^{-1}, l is the length of the effective lever arm in mm and $\tau(\theta)$ is torque as a function of joint angle calculated as:

$$\tau(\theta) = \theta\cdot(\tau_{start}-\tau_{end})/(\theta_{start}-\theta_{end}) + \tau_{start} - (\tau_{start}-\tau_{end})/(\theta_{start}-\theta_{end})\cdot\theta_{start}\,, \qquad (3)$$

in which τ_{start} and τ_{end} are torque corresponding to the beginning and end of extension, respectively. This calculation approximates the actual relationship between torque and angular excursion as linear (Fig. 4D), and assumes constant animal speed. The lever arm was the distance between the joint axis and the point of leg contact with the substrate. We analyzed five video trials using four *Leiobunum* and four trials using four *Eremopus*. The work by the patella–tibia and tibia–basitarsus joints of *Eremopus* were summed to give the total potential work by elastic extension of the fourth leg.

Results

Magnitude of torque generated by joints with transarticular sclerites

Joints with transarticular sclerites extended elastically over the full range of motion. These joints were the patella–tibia and tibia–basitarsus joints of *Eremopus* and the tibia–basitarsus joints of *Leiobunum*. The patella–tibia joints of *Mastigoproctus* and the tibia–basitarsus joints of scorpions also extended elastically, and some sclerotization of the membrane of these joints was observed.

Patella–tibia joints of *Eremopus* (N=4, mass=1.4±0.4 g) were rotated through approximately 60–120° (Fig. 3). Elastic extension over the range measured by motion analysis occurred at 0 kPa. Torque increased with pressure, and pressurizing the patella–tibia joint (Fig. 4) to 4.9 kPa (37 mmHg) approximately doubled the extension torque at any angle. Torque at midrange (90°) generated by the patella–tibia joint was 6.4±2.4 mN mm at 0 kPa, 9.3±3.5 mN mm at 2.5 kPa, 12.3±5.1 mN mm at 4.9 kPa and 18±7.9 mN mm at 9.8 kPa. Scaled torques at midrange angles are shown in Fig. 5. Scaled midrange torque generated solely by the elastic mechanism of this joint was equivalent to that generated by *Aphonopelma* femur–patella joints at 2.5 and 4.9 kPa and by *Mastigoproctus* femur–patella joints at 9.8 kPa (Table 1, Fig. 5).

Tibia–basitarsus joints of *Eremopus* (N=4, mass= 1.3±0.48 g) were moved through ranges indicated by motion analysis (150–170°) (Fig. 3). Induced flexion of this joint could occur to angles of approx. 100° and therefore joints were also flexed to this angle, although this degree of flexion is

Table 1. *Means of scaled midrange torque for various joints and* P *values for differences between means*

			P values									
						Aphonopelma						
			Eremopus	*Leiobunum*	*Mastigoproctus*	Fe–Pa			Ti–Bt			*Heterometrus*
Joint	Pressure (kPa)	Mean (N=4)	Ti–Bt (0 kPa)	Ti–Bt (0 kPa)	Fe–Pa (9.8 kPa)	2.5 kPa	4.9 kPa	9.8 kPa	2.5 kPa	4.9 kPa	9.8 kPa	Fe–Pa (9.8 kPa)
Eremopus												
Pa–Ti	0	5.2	0.37	0.02	0.19	0.24	0.01	0.01	0.01	0.22	0.03	0.01
Ti–Bt	0	5.4		0.03	0.28	0.19	0.03	0.01	0.01	0.20	0.03	0.01
Leiobunum												
Ti–Bt	0	2.4			0.43	0.35	0	0.01	0.35	0.01	0.01	0
Mastigoproctus												
Fe–Pa	9.8	3.0				0.29	0	0.01	0.29	0.15	0.01	0.05
Aphonopelma												
Fe–Pa	2.5	4.1					0	0.01	0.04	0.73	0.01	0.01
Fe–Pa	4.9	7.8						0.03	0	0	0.32	0
Fe–Pa	9.8	15.6							0.01	0.01	0.04	0
Ti–Bt	2.5	2.1								0	0	0.01
Ti–Bt	4.9	4.3									0.02	0
Ti–Bt	9.8	9.1										0
Heterometrus												
Fe–Pa	9.8	0.4										

Means were subjected to a two-tailed t-test, unequal variance; P<0.05 indicates a significant difference between the means.
Fe–Pa, femur–patella joint; Pa–Ti, patella–tibia joint; Ti–Bt, tibia–basitarsus joint.

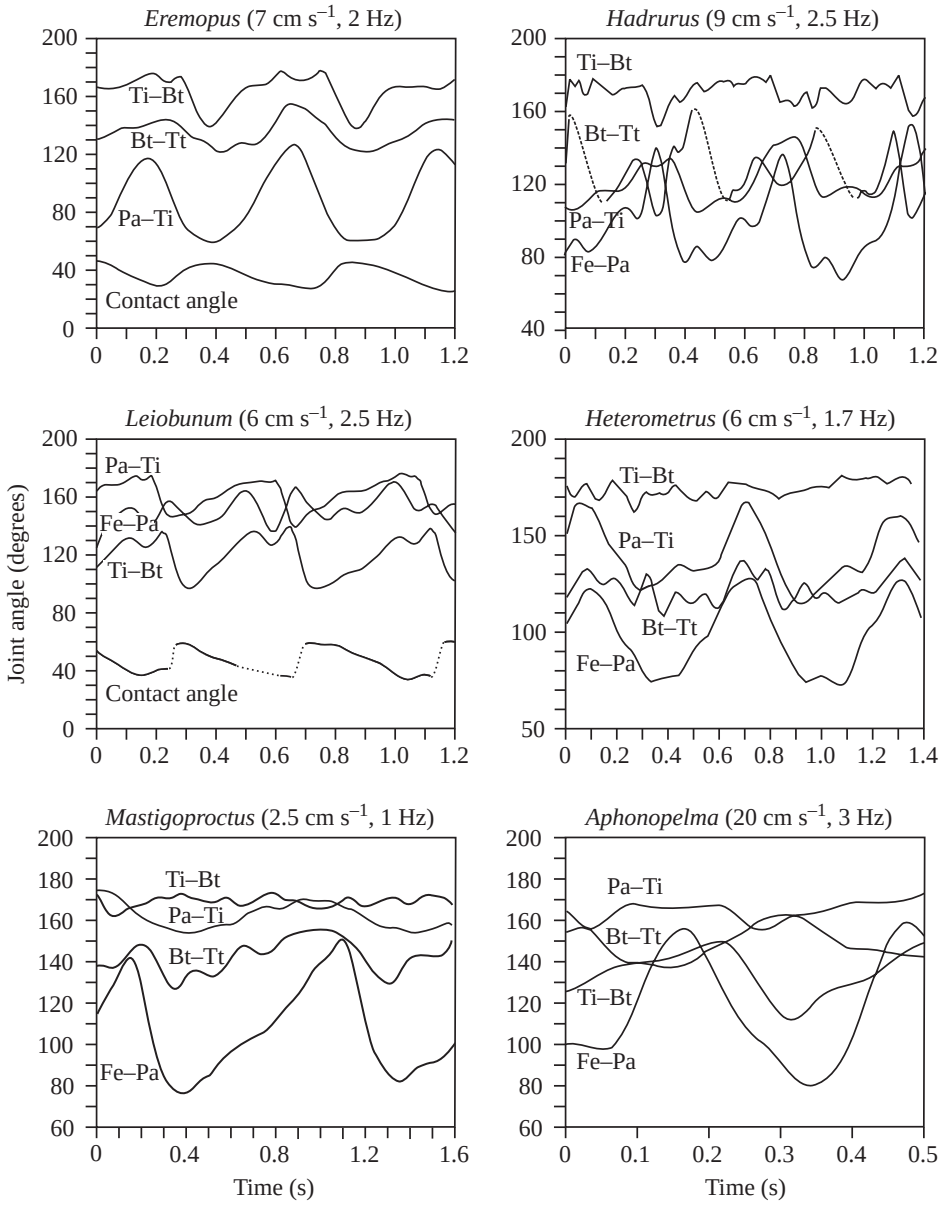

Fig. 3. Changes in joint angles during walking at typical speeds (representative trials). Speed and step frequencies are noted in parentheses. The contact angle depicted for *Eremopus* and *Leiobunum* is the projection onto the sagittal plane of the angle between the substratum and lever arm and was used to calculate potential propulsive work due to elastic recoil. Dotted lines are inferred due to incomplete kinematic information. The basitarsus–telotarsus joint angle is diagrammed as the supplementary angle. Fe–Pa, femur–patella joint; Pa–Ti, patella–tibia joint; Ti–Bt, tibia–basitarsus joint; Bt–Tt, basitarsus–telotarsus joint.

substantially greater than that observed during locomotion. Elastic extension at 0 kPa occurred not only over the range measured in walking animals but also after much greater flexion. Pressurizing the tibia–basitarsus joint (Fig. 4) to 4.9 kPa (37 mmHg) increased the torque by approx. 20%. Torque at midrange (160°) generated by the tibia–basitarsus joint was 6.7±1.5 mN mm at 0 kPa, 8.2±1.9 mN mm at 2.5 kPa, 8.4±2.1 mN mm at 4.9 kPa and 13±2.2 mN mm at 9.8 kPa. Scaled midrange torque generated solely by the elastic mechanism of this joint was equivalent to that generated by *Aphonopelma* tibia–basitarsus joint at 4.9 kPa (Table 1, Fig. 5).

The tibia–basitarsus joints of *Leiobunum* (*N*=4, mass=71±6 mg) were rotated through 100–150° (Fig. 3). Joints were also rotated through ranges as great as 90–170°. Elastic extension occurred over the entire range measured by motion analysis. Pressurizing the joint to 9.8 kPa (74 mmHg) raised peak torque by approx. 15% (Fig. 4). Torque generated by the tibia–basitarsus joint at midrange (125°) was 0.45±0.05 mN mm at 0 kPa, 0.47±0.05 mN mm at 4.9 kPa and 0.50±0.06 mN mm at 9.8 kPa. Scaled midrange torque generated by the elastic mechanism of this joint was equivalent to that generated by hydraulic pressure in *Aphonopelma* tibia–basitarsus joint at 2.5 kPa but less than that generated by the elastic mechanism of *Eremopus* tibia–basitarsus joints (Table 1).

Narrow strips of sclerotization span the arthrodial membrane of the patella–tibia joint of *Mastigoproctus* and this structure appeared to store and release some energy by folding. The patella–tibia joint of *Mastigoproctus* (*N*=3, mass=6±2 g) was elastic over the range used by walking animals, with resilience as great as 80% (Fig. 6). Excursion of this joint was small, and the lack of resolution in determining joint angle made accurate simulation of the walking range difficult. The maximum torque measured at this joint was high, with one specimen generating torque up to approx. 300 mN mm within the walking range. Torque generated by the patella–tibia joint at midrange (155°) was 13±6 mN mm at 0 kPa, 15±5 mN mm at 2.5 kPa, 19±2 mN mm at 4.9 kPa and 24±6 mN mm at 9.8 kPa. Variance of scaled midrange torque among individuals was high.

The tibia–basitarsus joints of both scorpion species were compliant and resilient when flexed over the inducible range of approximately 160–185° (Fig. 7). Scorpions typically rested with this joint hyperextended (approximately 200°), and when flexed, the elastic mechanism exerted a torque that resisted flexion and stored energy. The tibia–basitarsus joint appeared to be the only leg joint in scorpions with some sclerotization

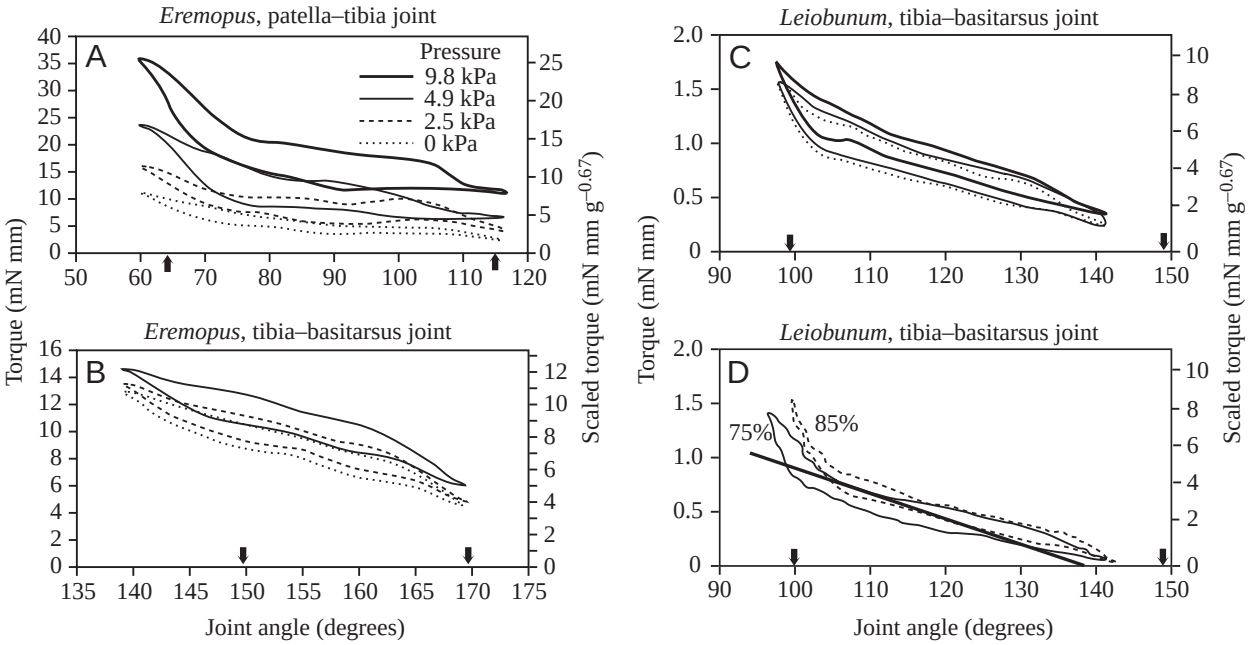

Fig. 4. Torque generated by isolated joints of representative *Eremopus* and *Leiobunum* during simulated locomotor cycles. Arrows denote the mean limits of joint excursion measured in walking animals. (A–C) Different internal fluid pressures. (D) Two work loops generated by tibia–basitarsus of *Leiobunum* at 0 kPa representing typical variation between frequencies and individuals. The heavy line represents the approximation of torque used in the calculation of elastic recoil to forward motion. Values of resilience (%) are shown next to the corresponding work loop.

of the arthrodial membrane. Movement of the tibia–basitarsus joint was difficult to resolve by video recordings due to a small excursion range. Observations of slow walking suggested that the elastic mechanism of this joint is loaded during the propulsive stroke. The tibia–basitarsus joint flexes during propulsion, but only to approx. 180°. Over the induced range, maximum torque generation was approx. 120 mN mm (Fig. 7) and resilience was approx. 70%.

Magnitude of torque generated by joints without transarticular sclerites

Joints without transarticular sclerites never extended elastically over any significant excursion range. These joints were the femur–patella and patella–tibia joints of scorpions, and the femur–patella and tibia–basitarsus joints of *Aphonopelma*. The femur–patella and tibia–basitarsus joints of *Mastigoproctus*, while weakly sclerotized, were also very limited in elastic extension.

Induced flexion of the femur–patella and patella–tibia joints of both scorpion species was achieved by torque lower than 10 mN mm over this range, and little extension occurred when the joint was moved away from the transducer's input tube (Fig. 7). Pressure of 9.8 kPa (74 mmHg) in both these joints resulted in limited extension, much less than that observed in walking. The patella–tibia joints of *Heterometrus* and the femur–patella and patella–tibia joints of *Hadrurus* produced no torque at midrange angles at pressures up to 9.8 kPa. Torque generated by the femur–patella joint of *Heterometrus* at midrange (100°) was 1.3±0.58 mN mm at 9.8 kPa. Scaled midrange torque in the femur–patella and patella–tibia joints of scorpions generated by hydraulic pressure of 9.8 kPa was significantly lower than that generated in the femur–patella and patella–tibia joints of all other species at the same pressure.

The femur–patella and tibia–basitarsus joints of *Aphonopelma* (N=4, mass=16±5 g) did not extend elastically over the range observed in locomotion, but an internal pressure of 4.9 kPa (37 mmHg) was usually sufficient to induce full extension. Pressurization readily induced higher torque in all these joints. Torque generated by the femur–patella joint at midrange (120°) was 28±14 mN mm at 25 kPa, 52±16 mN mm at 4.9 kPa and 98±34 mN mm at 9.8 kPa. Torque generated by the tibia–basitarsus joint at midrange (140°) was 14±7 mN mm at 25 kPa, 29±7 mN mm at 4.9 kPa and 60±18 mN mm at 9.8 kPa.

The femur–patella joint of *Mastigoproctus* (N=4, mass=6±1.4 g) resisted loading at maximum induced flexion, but resilience was low (approx. 18%) and could not extend the joint beyond approx. 10°. Pressure lower than 4.9 kPa (37 mmHg) was never sufficient to cause the degree of extension observed in walking (Fig. 6). Torque generated by the femur–patella joint at midrange (105°) was 2±1.7 mN mm at 25 kPa, 4±2.4 mN mm at 4.9 kPa and 10±5.8 mN mm at 9.8 kPa.

The tibia–basitarsus joints of *Mastigoproctus* were elastic only over the lower range of angles used in walking (Fig. 6). However, flexion beyond this walking range resulted in elastic extension, and resilience as high as 80% was measured. At this high degree of flexion, pressure of 49 kPa (37 mmHg) raised peak torque by approx. 25%.

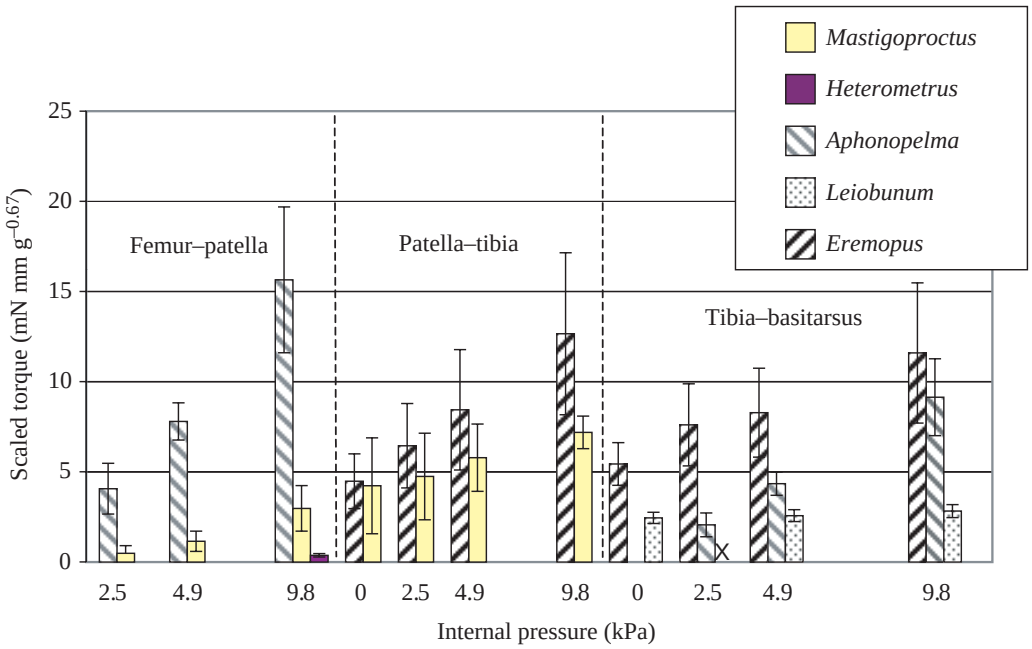

Fig. 5. Scaled midrange torques at applied internal fluid pressures. Midrange torques are those torques generated by a joint at an angle located midway between the maximum and minimum angles observed during locomotion. Values are means ± 2 S.E.M. X indicates that measurements were not taken. No torque was generated by the femur–patella joint of *Hadrurus* or by the patella–tibia joints of both scorpion species at all pressures tested.

Time-dependent effects on resilience and torque

The resilience of joints with obvious elastic properties was measured at different frequencies. Patella–tibia joints of *Eremopus* operated with resilience of 83±6% over frequencies of 0.5 to 5 Hz, and the changes in resilience and torque at different frequencies were smaller than typical experimental variation and displayed no consistent trends. The frequency of 10 Hz resulted in substantial vibration in the joint and noise in the data, and resilience appeared to decrease. However, resilience was never observed to be lower than 70%. Measurement of *Eremopus* tibia–basitarsus joints and *Leiobunum* tibia–basitarsus joints produced similar results with *Eremopus* operating with resilience of 85±11% and *Leiobunum* with resilience of 82±9% (Fig. 4) across frequencies of 0.5 to 5 Hz. No consistent dependence on frequency or angular excursion was apparent.

While no time–dependent properties were measured during constant cycling, the recoil force of *Eremopus* elastic joints held at a constant angle decayed after loading, with the initial loss of force being especially rapid (Fig. 8). When flexed to an angle normally seen in locomotion, the extension force of the patella–tibia joint of *Eremopus* dropped by approx. 30% of its original magnitude after 0.4 s and then underwent a slower decay for many seconds thereafter. When flexed and held at angles used in locomotion and greater, the force exerted by the tibia–basitarsus joint decayed by 10–15% after 0.3 s. After 13 s the extension force was at least 80% of its original magnitude (Fig. 8). The decay in recoil force of the tibia–tarsus joint of *Leiobunum* at maximum flexion tended to be greater than that of the patella–tibia joint of *Eremopus*, with the fast (0.5 s) initial loss in force being 30–50% (Fig. 8).

Centrifugal forces involved in motion of the steel tube prevented reliable measurement of torque and resilience at high frequencies (≥5 Hz) in joints that extended only under hydraulic pressure (e.g. tibia–basitarsus and femur–patella joints of *Aphonopelma* and femur–patella joints of *Mastigoproctus*).

Contribution by elastic mechanisms to forward locomotion

Combining the data from video recordings and kinetic studies, elastic recoil within a fourth leg of *Eremopus* had the potential to perform 7±1 μJ g^{-1} body mass and *Leiobunum* 3.3±0.5 μJ g^{-1} body mass of mechanical work during a step cycle. A study of energy changes during running in the cockroach *Blaberus discoidalis* (average mass 2.6 g, speed 240 mm s^{-1}) measured a total energy increase of approx. 20 μJ during a step cycle, representing mechanical work of 7.7 μJ g^{-1} body mass (Full and Tu, 1990).

Torque generated by basi–telotarsus joints

The basi–telotarsus joints of all the arachnids used in this study moved through a hyperextended range (Table 2) and exhibited elastic recoil after flexion, although torque was much lower than that measured in more proximal elastic joints or proximal joints activated by hydraulic pressure. The basitarsus–telotarsus joints of *Mastigoproctus* generated maximum torque of approx. 0.1 mN mm in the range used during locomotion. The basitarsus–telotarsus joints of scorpions, which move in a complicated manner, generated maximum torque of approx. 20 mN mm. The multiply segmented tarsus of *Leiobunum* was elastic and flexible, and the tarsus was flexed approx. 50°. Maximum torque by elastic extension was 0.04 mN mm. The basitarsus–telotarsus joint of *Aphonopelma* extended elastically (Fig. 6), with maximum torque in the walking range of approx. 5 mN mm. This joint also appeared to easily transduce pressure into torque.

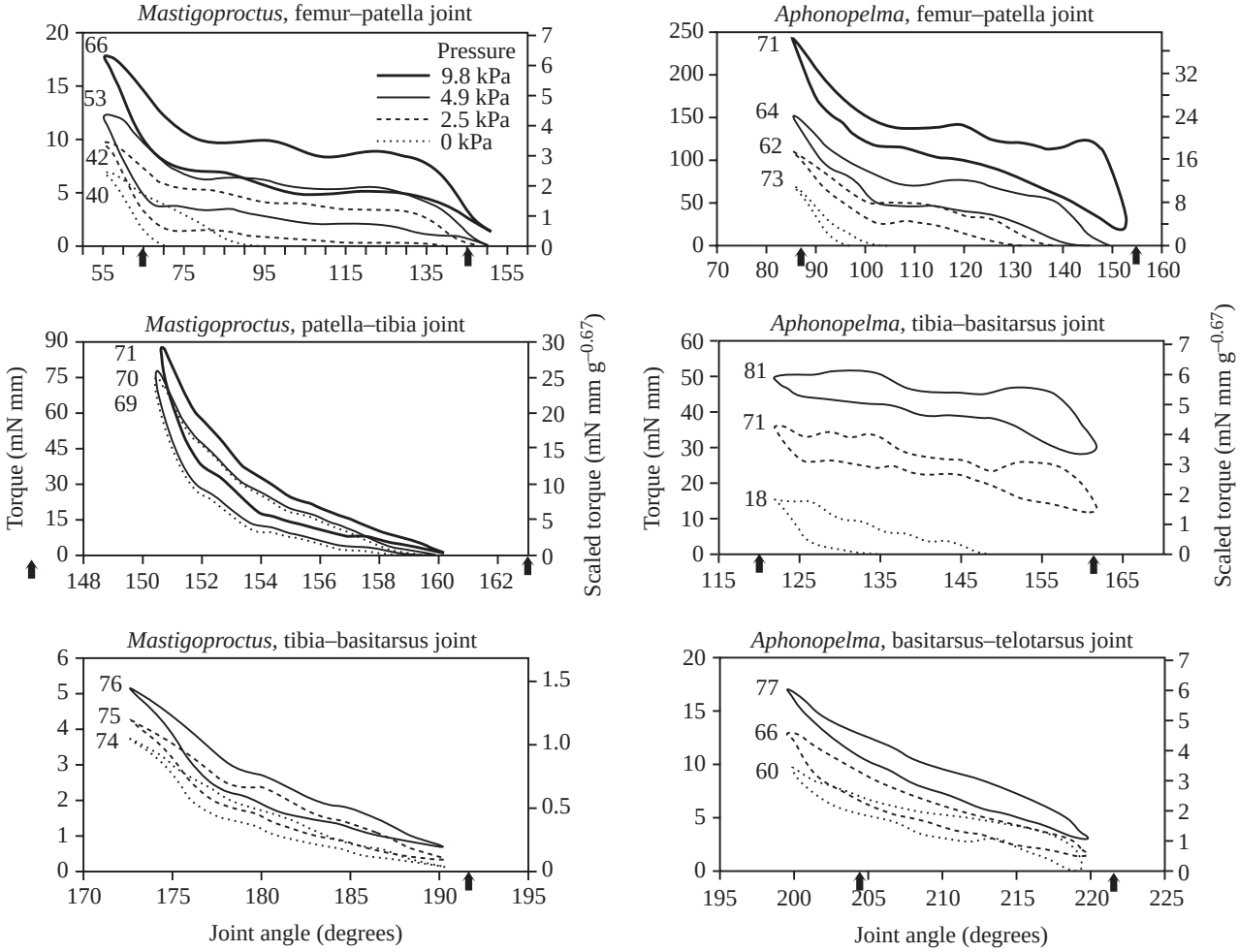

Fig. 6. Torque generated by isolated joints of representative *Mastigoproctus* and *Aphonopelma* during a simulated locomotor cycle under different internal fluid pressures. Values of resilience (%) are shown next to the corresponding work loop. Arrows denote the mean limits of joint excursion measured in walking animals.

Discussion

Mechanics of leg extension in arachnids

Hydraulic extension has been well documented in spiders and whipscorpions. Pressures up to 9 kPa have been measured in walking *Mastigoproctus* (Shultz, 1991) and from 5.3 to 8 kPa in *Aphonopelma* (Stewart and Martin, 1974). The pressure used for joint extension is apparently generated by compression of the prosoma by dorsoventral muscles (Shultz, 1991) and is maintained at elevated levels throughout locomotor activity (Wilson and Bullock, 1973; Stewart and Martin, 1974; Anderson and Prestwich, 1975; Shultz, 1991). The present study showed that the pressure previously measured in the legs is sufficient to generate substantial torque. As in the femur–patella and tibia–basitarsus joints of the spider *Tegenaria* (Parry and Brown, 1959a), torque increased approximately linearly with pressure (Fig. 5). Torque measured in the present study in amputated tibia–basitarsus joints of the tarantula *Aphonopelma* (20–74 mN mm) over the range 2.5–9.8 kPa was similar to torque generated by this joint in live, restrained *Cupiennius*, a similar–sized spider (Blickhan and Barth, 1985). Very high pressures have been measured in the legs of restrained spiders (63 kPa) (Stewart and Martin, 1974) and scorpions (33 kPa) (Alexander, 1967), but it is thought that these pressures are not normally used in walking (Alexander, 1967). Jumping spiders may use very high pressures to rapidly extend the rear legs during a jump (Parry and Brown, 1959b).

Differences in joint morphology also correlate with differences in magnitude of the torque generated by pressure. Unlike the bellows-like folding of the femur–patella and tibia–basitarsus joints of *Aphonopelma*, the arthrodial membrane of the femur–patella joint of *Mastigoproctus* tends to bulge under pressure. Bulging of the arthrodial membrane can hinder extension because stresses are not resolved radially (Blickhan and Barth, 1985) and may be an explanation for the lower relative torque generation in *Mastigoproctus*. Joints extended by haemolymph pressure are characterized by internal volume change during joint rotation and a center of gravity not located at the rotational axis (Blickhan and Barth, 1985). Internal volume changes for some joints were large

Table 2. *Joint excursions, speeds and frequencies of walking arachnids*

	Taxon					
	Eremopus	*Leiobunum*	*Aphonopelma*	*Mastigoproctus*	*Heterometrus*	*Hadrurus*
Individuals	6	4	4	4	5	5
Trials	19	20	11	9	9	11
Body mass (g)	1.4±0.4	0.071±0.014	16±2	5.5±1.8	7.0±1.5	6.9±1.2
Speed range (mm s^{-1})	72–320	33–88	60–700	15–59	35–107	35–77
Step frequency range (Hz)	2.0–7.1	1.7–3.1	1–8.3	0.8–1.7	1.2–3.1	1.1–2.5
Range of joint angles (°)						
Femur–patella joint	–	142±6–167±6	87±10–158±9	64±7–144±10	70±6–126±9	67±6–124±11
Patella–tibia joint	65±8–115±16	153±4–171±3	151±7–168±6	144±5–163±6	112±9–151±10	109±6–159±10
Tibia–basitarsus joint	149±8–170±7	103±9–150±8	119±15–162±7	218±12–192±7	–	–
Basitarsus–telotarsus joint	232±9–209±8	–	222±5–205±8	232±9–207±7	223±8–248±9	228±10–253±10

Values for body mass are means ± S.D.
–, not measured by video analysis.
Range = mean minimum angle ± S.D. – mean maximum angle ± S.D.

Table 3. *Joint volume change during simulated joint movement*

	Eremopus	*Hadrurus*	*Heterometrus*	*Mastigoproctus*	*Aphonopelma*
Body mass (g) (mean ± S.D.)	1.14±0.22	6±1	6.0±1.9	8±2	18±2
Volume change (µl)					
Femur–patella joint	–	1±0.5l	1±0.5	3.5±1	20±3
Patella–tibia joint	2.5±1	<0.5	<0.5	<0.5	1±2
Tibia–basitarsus joint	<0.5	<0.5	<0.5	<0.5	8±2
Basitarsus–telotarsus joint	<0.5	<0.5	<0.5	<0.5	1±0.5

N=3 for all genera.
–, volumes not measured.

enough to measure using our technique (Table 3). The femur–patella joints of scorpion and *Mastigoproctus*, while similar in segmental dimensions, differed both in volume change and in location of the center of gravity. The volume change of femur–patella joints of *Mastigoproctus* is about three times greater than scorpions. The axis of joint rotation of femur–patella joints of scorpions is located near the middle of the limb and contrasts with the dorsally located axis of the femur–patella joints of *Mastigoproctus* (Fig. 1). Both the femur–patella and patella–tibia joints of scorpions appear to be extended by the transpatellar muscle (Shultz, 1992), and the role of pressure in extension of these joints is trivial or absent (Fig. 7).

Different extension mechanisms need not be exclusive, and indeed joints of *Mastigoproctus* display features of both hydraulic and elastic extension. These two mechanisms are probably synergistic in the femur–patella, patella–tibia, and tibia–basitarsus joints of *Mastigoproctus*. The mainly hydraulic femur–patella joint is proximal to the greatly elastic patella–tibia joint, and both joints have some sclerotization of the arthrodial membrane. Hydraulic pressure may be present in the patella–tibia joint at all times or, if the animal has a method of regulating pressure between joints, only during times of very high torque demand. *Mastigoproctus*, with its combination of hydraulic and elastic features, demonstrates the functional viability of an intermediate in the transition from dependence on hydraulic pressure to cuticular elasticity.

Eremopus probably represents an extreme example of dependence on cuticular elasticity for extension. While torque also increases with pressure in the patella–tibia and tibia–basitarsus joints of *Eremopus*, it is not known if such pressures are used in these animals. Walking pressures in *Eremopus* and *Leiobunum* have not been reported but are probably low due to a reduction of prosomal dorsoventral muscles (Shultz, 1991). Torque at the tibia–tarsus joint of *Leiobunum* increases very little as pressure is increased, and this is associated with the small change in joint volume during movement.

Elastic extension in *Eremopus* and *Leiobunum* appears to have replaced the hydraulic system seen in *Aphonopelma* and *Mastigoproctus* (Shultz, 1990, 1991). The femur–patella joint of *Aphonopelma* and *Mastigoproctus* and the patella–tibia joint of *Eremopus* are functionally similar ‘knee’ joints of the fourth leg and are assumed to be the main contributors to propulsion by this leg. Elastic extension alone produces a midrange scaled torque of 5.2±0.8 mN mm $g^{-0.67}$ in the patella–tibia joint of

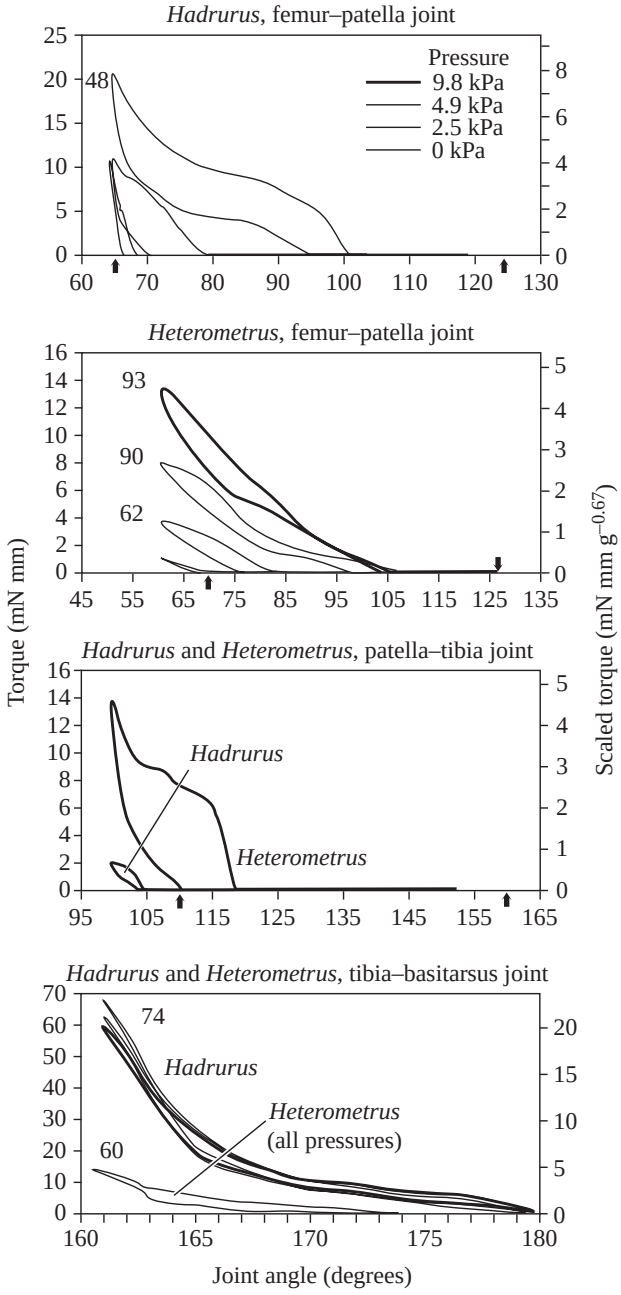

Fig. 7. Torque generated by isolated joints of representative *Hadrurus* and *Heterometrus* during a simulated locomotor cycle under different internal fluid pressures. Values of resilience (%) are shown next to the corresponding work loop. Arrows denote the mean limits of joint excursion measured in walking animals.

Eremopus, while the femur–patella joints of *Aphonopelma* and *Mastigoproctus* generate no torque except when pressurized. The femur–patella joint of *Aphonopelma* required between 0 and 2.5 kPa of pressure and the femur–patella joint of *Mastigoproctus* greater than 4.9 kPa to produce scaled torque comparable to the elastic extension in *Eremopus*. These measurements suggest that torque generated by elastic extension alone may be sufficient for walking in *Eremopus*. Scaled midrange torque of the tibia–tarsus joint of *Leiobunum* is lower than other joints with sclerites, and this may be partly due to its distal location on the leg. The elastically generated scaled torque at this joint is similar to the scaled torque produced by the femur–patella joint of *Mastigoproctus* at its typical walking pressures. Both *Leiobunum* and *Mastigoproctus* tended to use lower speeds than *Eremopus* and *Aphonopelma*, and this may associated with the lower torques observed in the joints.

Elastic joint extension may be an evolutionarily simple way of replacing the ancestral hydraulic mechanism (Shultz, 1989, 1991) and its potentially disruptive impact on haemolymph circulation. The pressure used for joint extension can potentially impede the transport of oxygenated haemolymph from opisthosomal respiratory organs to the locomotor muscles of the prosoma. Any cost of the hydraulic mechanism could be reduced by shifting the role of joint extension to some mechanism intrinsic to the leg, such as an extensor muscle or transarticular elastic sclerite. The thickening of the pre-existing arthrodial membrane to form a transarticular sclerite would seem relatively easy to evolve in comparison to the multiple innovations necessary to generate a new muscle and a neural mechanism for controlling it. The continuous resistance of an elastic mechanism to contraction of flexor muscles would be mechanically similar to that caused by constant elevated haemolymph pressure during locomotion, as illustrated by a comparison of the loading curves of elastic joints of *Eremopus* and *Leiobunum* (Fig. 4) to those of the hydraulic joints of *Aphonopelma* (Fig. 6). Further, the energy exerted by flexor muscles to maintain a posture at hydraulic joints during inactivity is reduced in *Aphonopelma* and *Mastigoproctus* by lowering internal pressure below levels observed during walking (Stewart and Martin, 1974; Shultz, 1991), and a comparable effect is achieved at elastic joints of *Eremopus* and *Leiobunum via* gradual viscoelastic decay in torques exerted by transarticular sclerites, although this decay still leaves significant torque remaining in the joint (Fig. 8).

The stiffness of a joint in live animals is determined by membrane structure, fluid pressure and muscle properties. The dorsal–ventral stiffness of the tibia–basitarsus joint of live *Aphonopelma* was measured by Blickhan (1986). To determine the stiffness of the membrane apart from the effects of muscles and hydraulic fluid, excursion was limited to several degrees and low frequency (<0.1 Hz). Stiffness measured in that study was essentially the same as that measured at midrange (slope of the torque *versus* angle curve at midrange) during hydraulic extension in the present study, approx. 0.01 mN degree^{-1}. However, flexion of several degrees at a frequency of 0.1 Hz in the live spider in Blickhan's (1986) study resulted in a stiffness increase of several hundredfold. This high stiffness was probably the result of muscle tension. Intrinsic stiffness of the membrane is probably insignificant in operation over most of the excursion range of hydraulically extended joints, and stiffness in live animals is primarily determined by hydraulic pressure and muscle tension. At high flexion, however, joint stiffness increases as a result of compression of the membrane, transarticular sclerite or limb cuticle. All of the 'knee joints'

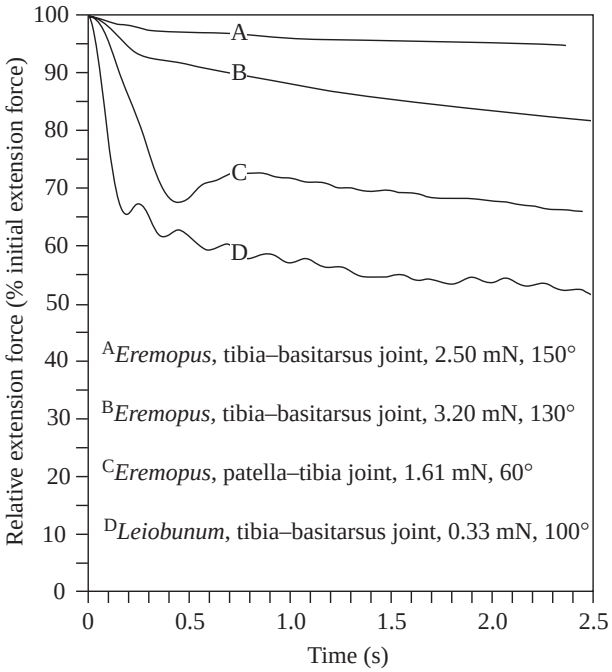

Fig. 8. Decay in extension force of elastic joints over time. Each joint was flexed and maintained in a flexed position while recording torque. The absolute magnitudes of initial torque and joint angle are noted.

and the tibia–basitarsus joint of *Leiobunum* operate close to or at the flexion limit during normal walking, as indicated by the increase in stiffness near the end of flexion during the simulated walking cycles (Figs 4, 6, 7). The tibia–basitarsus joints of *Eremopus* and *Aphonopelma* do not appear to operate near the flexion limit during normal walking (Figs 4, 6).

The resilience of the transarticular sclerite during leg rotation in arachnids is in the range of that measured for elastic proteins such as elastin (76%), abductin (91%) and resilin (97%) (Wainwright et al., 1976; Vincent, 1982). Resilin has been identified at several structures in insects, including the jumping mechanism of the flea (Bennet-Clark and Lucey, 1967) and click beetle (Sannasi, 1969), the tibia and tarsus of the cockroach (Frazier et al., 1999; Neff et al., 2000) and the wing base of dragonflies (Weis-Fogh, 1960, 1965). While elastic structures in insects are usually loaded by compression and bending forces operating through a small distance in contrast to the extensive folding mechanism of the transarticular sclerites of arachnids, it is possible that the sclerites of arachnids do achieve relatively high resilience through incorporation of resilin. Alexander (1967) has proposed the existence of resilin in the femur–patella joint of the scorpion pedipalp, and this protein has been identified in the cuticle of the chelal hinge of scorpions (Govindarajan and Rajulu, 1974). Resilin or similar elastic proteins may be widely distributed among arachnids, and incorporated into both the transarticular sclerites and the basitarsus–telotarsus joint.

Arachnid joint springs compared to the spring-loaded inverted pendulum model

Elastic energy storage is well known as a mechanism for increasing energetic efficiency in running vertebrates, and the simplest model is known as the spring-loaded inverted pendulum (SLIP) (Cavagna et al., 1977; Heglund et al., 1982; McMahon, 1985, 1990; Alexander, 1984, 1988, 1992; Blickhan, 1989; Thompson and Raibert, 1989; McMahon and Cheng, 1990; Full 1989; Farley et al., 1993). During the first cycle in a running sequence, the body is accelerated upward and forward by muscles. As the legs interrupt the body's fall back toward the substratum, the legs absorb mechanical energy from the impact and store some of it as elastic deformation in tensed tendons and muscles. The ground reaction forces may be several times the body weight during running (Farley et al., 1993). Subsequent recoil of elastic elements then assists muscles in accelerating the body upward and forward at the start of the next locomotor cycle. Thus some of the muscular energy generated during one cycle is stored in elastic elements and used in the next cycle.

The SLIP model requires leg springs to be located so that the falling center of mass can compress the spring. However, most arthropods maintain a 'bent-leg' hanging posture with legs projecting radially around the center of mass, rather than a typical vertebrate 'straight-leg' posture with legs positioned below the center of mass (Manton, 1977; Alexander, 1982). Though the motion of the center of mass of certain cockroaches, crabs and centipedes suggests that they are using a leg spring in the manner predicted by the SLIP model (Full, 1989; Blickhan and Full, 1993; Full and Koditschek, 1999), the transarticular springs in arachnid joints do not appear to be oriented so as to be readily compressed by the center of mass. Instead, the elastic mechanisms of *Eremopus* and *Leiobunum* are apparently loaded by flexor muscles during protraction, the phase of the step cycle when the leg is not in contact with the substratum. The energy stored during this period is then recovered when the leg is in contact with the substratum and has the potential to make a substantial contribution to propulsion. The mechanical energy inputs calculated for *Eremopus* ($7\pm1\,\mu J\,g^{-1}$ body mass) and *Leiobunum* ($3.3\pm0.5\,\mu J\,g^{-1}$ body mass) are comparable to those of arthropods that rely on muscle-based joint extension. For example, the cockroach *Blaberus discoidalis* performs mechanical work of approx. $8\,\mu J\,g^{-1}$ body mass during one step cycle (based on Full and Tu, 1990). Thus, elastic storage mechanisms exist in small arthropods and can potentially generate substantial thrust during walking and running.

Potential advantages of elastic mechanisms in running arthropods

The use of elastic extension by some arachnids requires explanation in light of its deviation from the SLIP model and its apparent evolutionary derivation from an ancestral hydraulic mechanism (Shultz, 1989, 1990, 1991). We propose three possible advantages of elastic energy storage during walking and running in arthropods.

First, the use of elastic structures at leg joints instead of hydraulic fluid may reduce leg mass and inertia and increase energetic efficiency. While energetics did not differ between large vertebrates with very different limb inertias (Taylor et al., 1974), minimization of leg inertia is likely to be an important determinant of leg structure and mechanics in arthropods, which tend to use even higher stride frequencies (>25 Hz in *Periplaneta americana*; Full and Tu, 1991). For example, the cockroach mass-specific kinetic energy required to swing its legs is about half that predicted from data on larger two- and four-legged animals (Kram et al., 1997). Elastic mechanisms of the most distal joints are found in scorpions, whipscorpions, sun-spiders, tarantulas (A.T.S. and J.W.S., unpublished observation), cockroaches (Frazier et al., 1999), stick insects (Radnikov and Bassler, 1991), and probably other arthropods. The tibia–tarsus joint of scorpions appears to absorb energy during propulsion, since any loading of the membrane occurs during this phase. This is opposite to that seen in the main elastic joints of *Eremopus*, *Leiobunum*, and *Mastigoproctus*.

Second, elastic structures may reduce energetic costs associated with fluid displacement and pressure maintenance in hydraulic extension. Those arachnids using hydraulic extension show volume displacements of several μl per leg during each step cycle. Viscous drag of hydraulic fluid flow would be much greater in small limbs, assuming drag proportional to r^{-4} (Poiseuille's Law) and bulk proximal fluid flow during flexion and distal flow during extension. Extrapolating from volume displacements, a unit of fluid probably moves several mm during leg cycling, so that an assumption of bulk fluid flow is reasonable. Assuming that viscosity and velocity are similar in different arachnids, the relative importance of viscous drag can be estimated. Using the leg diameters of our experimental animals, *Eremopus* would have about 50 times the viscous drag of *Aphonopelma* and *Leiobunum* would have about 500 times the drag of *Aphonopelma*. Legs extended by hydraulic pressure would tend to have large diameters in order to reduce drag. The scorpion pedipalp *Aphonopelma* walking legs and *Mastigoproctus* walking legs, are relatively large in diameter and include at least one joint primarily activated by pressure. The patella–tibia joint of *Eremopus*, while extending by cuticular elasticity, has a relatively large diameter, and pressure in amputated preparations can contribute to extension torque. Not only is there potential for energy loss in fluid movement through limbs, but a hydraulic reservoir itself may contribute to inefficiency. A hydraulic system with an ideal reservoir could be perfectly elastic. The reservoir consisting of tubing and a column of solution used in the simulated walking of *Aphonopelma* and *Mastigoproctus* resulted in a hydraulic resilience that was very similar to the resilience produced by transarticular sclerites. The hydraulic reservoir (prosoma) of *Mastigoproctus* and *Aphonopelma* probably also loses a similar amount of energy to stretching of the haemocoel.

Third, elastic structures may act as passive mechanisms of energy absorption and dissipation. In the typical hanging stance of *Leiobunum*, destabilizing forces such as wind may be absorbed by elastic loading on the side opposite the disturbing force. With a roughly radial distribution of legs, the animal is thus equipped with a passive shock absorbing system that may respond quickly to destabilizing forces. The forces associated with loading and recoil of elastic mechanisms of the fourth leg are 5–20% of body weight in *Eremopus* and 5–10% of body weight in *Leiobunum*, and thus the ground reaction forces produced by a tipping animal are sufficient to load the elastic structures of a single leg beyond that observed in locomotion. While the hanging stance is especially exaggerated in the long-legged *Leiobunum*, it is a general characteristic of arthropods (Manton, 1977), and this mechanism may contribute to stability in other arthropods as well. The elastic torque generated by extreme flexion in the tibia-basitarsus of *Mastigoproctus* and scorpions and in the tarsus of *Leiobunum* probably functions as a shock absorber during climbing or other deviations from walking on smooth horizontal surfaces. High resilience of an elastic mechanism may not be desirable when it is functioning as an energy damper. Muscles can also act as dampers. During running, net energy is absorbed by the primary extensor muscles (trochanter–femur muscle) of the rear leg of the cockroach *Blaberus discoidalis* (Full et al., 1998), probably for control purposes. However, these cockroach muscle extensors are located close to the leg base and their movement and function are probably not comparable to the more distal elastic extensors of the arachnids studied here.

In conclusion, transarticular sclerites in arachnids are mechanisms of energy storage, and play a prominent role in leg extension in animals in which they occur. Hydraulic pressure is also an important component of locomotion in many arachnids, and may function in synergy with transarticular sclerites. The evolution of alternative extension mechanisms like elasticity and musculature from the hydraulically operated condition suggest adaptive benefits associated with these alternative mechanisms.

We thank Claudio Gratton for programming assistance. This work was funded through National Science Foundation Grant (IBN-9733777), Maryland Agricultural Experiment Station, and a University of Maryland Behavioral Ecology and Evolutionary Systematics grant.

References

Alexander, A. J. (1967). Problems of limb extension in the scorpion, *Opisthophthalmus latimanus* Koch. *Trans. R. Soc. S. Africa* **37**, 165-181.

Alexander, R. McN. (1982). *Locomotion in Animals*. New York: Chapman and Hall.

Alexander, R. McN. (1984). Elastic energy stores in running vertebrates. *Am. Zool.* **24**, 85-94.

Alexander, R. McN. (1988). *Elastic Mechanisms in Animal Movement*. Cambridge: Cambridge University Press.

Alexander, R. McN. (1992). A model of bipedal locomotion on compliant legs. *Phil. Trans. R. Soc. London B* **338**, 189-198.

Anderson, J. F. and Prestwich, K. N. (1975). The fluid pressure pumps of spiders (Chelicerata, Araneae). *Z. Morphol. Tiere* **81**, 257-277.

Bennet-Clark, H. C. (1975). The energetics of the jump of the locust, *Schistocerca gregaria*. *J. Exp. Biol.* **63**, 53-83.

Bennet-Clark, H. C. and Lucey, E. C. A. (1967). The jump of the flea: a study of the energetics and a model of the mechanism. *J. Exp. Biol.* **47**, 59-76.

Biewener, A. and Full, R. J. (1992). Force platform and kinematic analysis. In *Biomechanics – Structures and Systems* (ed. A. A. Biewener), pp. 45-73. New York: Oxford University Press.

Blickhan, R. (1986). Stiffness of an arthropod leg joint. *J. Biomech.* **19**, 375-384.

Blickhan, R. (1989). The spring-mass model for running and hopping. *J. Biomech.* **22**, 1217-1227.

Blickhan, R. and Barth, F. G. (1985). Strains in the exoskeleton of spiders. *J. Comp. Physiol.* **157**, 115-147.

Blickhan, R. and Full, R. J. (1993). Similarity in multilegged locomotion: bouncing like a monopode. *J. Comp. Physiol. A* **173**, 509-517.

Brodsky, A. K. (1994). *The Evolution of Insect Flight*. Oxford: Oxford University Press.

Cavagna, G. A., Heglund, N. C. and Taylor, C. R. (1977). Mechanical work in terrestrial locomotion: two basic mechanisms for minimizing energy expenditure. *Am. J. Physiol.* **233**, R243-R261.

Evans, M. E. G. (1972). The jump of the click beetle (Coleoptera: Elateridae) – a preliminary study. *J. Zool.* **167**, 319-336.

Evans, M. E. G. (1973). The jump of the click beetle (Coleoptera: Elateridae) – energetics and mechanics. *J. Zool.* **169**, 181-194.

Evans, M. E. G. and Forsythe, T. G. (1984). A comparison of adaptations to running, pushing and burrowing in some adult Coleoptera: especially Carabidae. *J. Zool. Lond.* **202**, 513-534.

Farley, C. T., Glasheen, J. and McMahon, T. A. (1993). Running springs: speed and animal size. *J. Exp. Biol.* **185**, 71-86.

Frazier, S. F., Larson, G. S., Neff, D., Quimby, L., Carney, M., DiCaprio, R. A. and Zill, S. N. (1999). Elasticity and movements of the cockroach tarsus in walking. *J. Comp. Physiol. A* **185**, 157-172.

Full, R. J. (1989). Mechanics and energetics of terrestrial locomotion: bipeds to polypeds. In *Energy Transformation in Cells and Organisms* (ed. W. Weiser and E. Gnaiger), pp. 175-182. Stuttgart: Georg Thieme Verlag.

Full, R. J. and Koditschek, D. E. (1999). Templates and anchors: neuromechanical hypotheses of legged locomotion on land. *J. Exp. Biol.* **202**, 3325-3332.

Full, R. J., Stokes, D. R., Ahn, A. N. and Josephson, R. K. (1998). Energy absorption during running by leg muscles in a cockroach. *J. Exp. Biol.* **201**, 997-1012.

Full, R. J. and Tu, M. S. (1990). Mechanics of six-legged runners. *J. Exp. Biol.* **148**, 129-146.

Full, R. J. and Tu, M. S. (1991). Mechanics of a rapid running insect: two-, four-, and six-legged locomotion. *J. Exp. Biol.* **156**, 215-231.

Govindarajan, S. and Rajulu, G. S. (1974). Presence of resilin in a scorpion *Palamnaeus swammerdami* and its role in the food-capturing and sound-producing mechanism. *Experientia* **15**, 908-909.

Heglund, N. C., Cavagna, G. A. and Taylor, C. R. (1982). Energetics and mechanics of terrestrial locomotion. III. Energy changes of the center of mass as a function of speed and body size in birds and mammals. *J. Exp. Biol.* **97**, 41-56.

Ingham, P. W. and Jowett, T. (1997). Localization of RNA transcripts by in situ hybridization. In *The Molecular Biology of Insect Disease Vectors* (ed. J. M. Crampton, C. B. Beard and C. Louis), pp. 268-282. London: Chapman and Hall.

Kram, R., Wong, B. and Full, R. J. (1997). Three-dimensional kinematics and limb kinetic energy of running cockroaches. *J. Exp. Biol.* **200**, 1919-1929.

Manton, S. M. (1977). *The Arthropoda*. London: Clarendon Press.

McMahon, T. A. (1985). The role of compliance in mammalian running gates. *J. Exp. Biol.* **115**, 263-282.

McMahon, T. A. (1990). Spring-like properties of muscles and reflexes in running. In *Multiple Muscle Systems* (ed. J. M. Winters and S. L.-Y. Woo), pp. 578-590. New York: Springer-Verlag.

McMahon, T. A. and Cheng, G. C. (1990). The mechanics of running: how does stiffness couple with speed? *J. Biomech.* **23(Suppl. 1)**, 65-78.

Neff, D., Frazier, S. F., Quimby, L., Wang, R.-T. and Zill, S. (2000). Indentification of resilin in the leg of cockroach, *Periplaneta americana*: confirmation by a simple method using pH dependence of UV fluorescence. *Arthropod Struct. Dev.* **29**, 75-83.

Parry, D. A. and Brown, R. H. J. (1959a). The hydraulic mechanism of the spider leg. *J. Exp. Biol.* **36**, 423-433.

Parry, D. A. and Brown, R. H. J. (1959b). The jumping mechanism of salticid spiders. *J. Exp. Biol.* **36**, 654-664.

Radnikov, G. and Bassler, U. (1991). Function of a muscle whose apodeme travels through a joint moved by other muscles: why the retractor unguis muscle in stick insects is tripartite and has no antagonist. *J. Exp. Biol.* **157**, 87-99.

Sannasi, A. (1969). Resilin in the cuticle of a click beetle. *J. Georgia Entomol. Soc.* **4**, 31-32.

Shultz, J. W. (1989). Morphology of locomotor appendages in Arachnida: evolutionary trends and phylogenetic implications. *Zool. J. Linn. Soc.* **97**, 1-56.

Shultz, J. W. (1990). Evolutionary morphology and phylogeny of Arachnida. *Cladistics* **6**, 1-38.

Shultz, J. W. (1991). Evolution of locomotion in Arachnida: the hydraulic pressure pump of the giant whipscorpion, *Mastigoproctus giganteus* (Uropygi). *J. Morphol.* **210**, 13-31.

Shultz, J. W. (1992). Muscle firing patterns in two arachnids using different methods of propulsive leg extension. *J. Exp. Biol.* **162**, 313-329.

Stewart, D. M. and Martin, A. W. (1974). Blood pressure in the tarantula, *Dugesiella hentzi*. *J. Comp. Physiol.* **88**, 141-172.

Taylor, R. C., Shkolnik, A., Dmi'el, R., Baharav, D. and Borut, A. (1974). Running in cheetahs, gazelles, and goats: energy cost and limb configuration. *Am. J. Physiol.* **227**, 848-850.

Thompson, C. and Raibert, M. (1989). Passive dynamic running. In *International Symposium of Experimental Robotics* (ed. V. Hayward and O. Khatib), pp. 74-83. New York: Springer-Verlag.

Vincent, J. F. W. (1982). *Structural Biomaterials*. New York: Wiley.

Wainwright, S. A., Briggs, W. D., Curry, J. D. and Gosline, J. M. (1976). The protein rubbers. *Mechanical Design in Organisms*, pp. 114-119. Princeton: Princeton Universty Press.

Weis-Fogh, T. (1959). Elasticity in arthropod locomotion: a neglected subject, illustrated by the wing system of insects. *Proc. 15th Int. Congr. Zool.* **4**, 393-395.

Weis-Fogh, T. (1960). A rubberlike protein in insect cuticle. *J. Exp. Biol.* **37**, 889-907.

Weis-Fogh, T. (1965). Elasticity and wing movements in insects. In *Proceedings of the Twelvth International Congress on Entomology* (ed. P. Freeman), pp. 186-188. London: Regal Entomological Society.

Wilson, R. S. and Bullock, J. (1973). The hydraulic interaction between prosoma and opisthosoma in *Amaurobius ferox* (Chelicerata, Araneae). *Z. Morphol. Tiere* **74**, 221-230.